

Theory of Photon Bands in Three-Dimensional Periodic Dielectric Structures

S. Satpathy, Ze Zhang, and M. R. Salehpour

Department of Physics and Astronomy, University of Missouri-Columbia, Columbia, Missouri 65211

(Received 27 December 1989)

Recent experiments have found the existence of "photon bands" in periodic dielectric structures analogous to the electron bands in the solid. Using a plane-wave method, we study in the scalar-wave approximation the nature of the photon bands in structures where spherical "atoms" of dielectric constant ϵ_a are periodically arranged in a background dielectric ϵ_b . The scalar-wave calculation predicts gaps in the spectrum for ϵ_a/ϵ_b or $\epsilon_b/\epsilon_a \gtrsim 3$ or so. The nature and symmetry of the wave functions is also discussed.

PACS numbers: 41.10.Hv, 71.25.Cx, 84.90.+a

It is well known that the electron forms energy bands in periodic crystals. The deviation from the free-particle dispersion may be thought to be caused by the coherent interference of scattering of electrons from individual atoms. This leads to the formation of gaps and other characteristic aspects in the electron band structure. Analogously, any particle would coherently scatter and form energy bands in a medium that provides a periodic scattering potential with a length scale comparable to the wavelength of the particle. Specifically this should be true for the propagation of classical electromagnetic (EM) waves in periodic dielectric structures.¹

Some possible applications of EM wave scattering from a collection of scatterers have been pointed out in the literature. Of fundamental interest among these is the possibility of Anderson localization of EM waves in disordered dielectric structures,²⁻⁶ where the strong Coulomb-interaction effect entering the electron-localization problem is absent. A related problem is the localization of surface-plasmon-polariton modes on a rough metal surface⁷ and its role in the surface-enhanced Raman scattering and other surface optical phenomena. Kurizki and Genack⁸ have pointed out the strong modification of atomic and molecular properties in a volume of space where "vacuum fluctuations" are absent. Yablonovitch⁹ has proposed that spontaneous emission is forbidden in a situation where the photon gap overlaps with the electronic band edge.

That such "photon bands" exist in periodic structures has recently been demonstrated. In their experiment, Yablonovitch and Gmitter¹ fabricated a series of periodic dielectric structures out of low-loss dielectric materials using conventional machine tools. These structures contained typically 8000 "atoms" which were dielectric spheres or simply spherical cavities filled with air. Using microwave photons they observed the existence of a photonic band gap.

The scattering of EM waves follows the Maxwell equations which are vector equations. The vector equations are much more complex to solve. Exact solutions do exist in simple cases, for instance, the Mie problem¹⁰ of EM wave scattering from a single sphere. In this Letter we show that many important aspects of the ex-

perimental photon bands in periodic dielectric structures can be understood in terms of scattering of the scalar waves. The scalar-wave approach is also directly applicable to the scattering of acoustic waves, an area of equally active interest.

The scattering of a scalar wave $\Psi(\mathbf{r})$ from a periodic lattice of dielectric spheres is described by the Helmholtz wave equation

$$\{-\nabla^2 - (\omega^2/c^2)\epsilon_b + V(\mathbf{r})\}\Psi(\mathbf{r}) = 0, \quad (1)$$

with

$$V(\mathbf{r}) = \frac{\omega^2}{c^2} \sum_{\mathbf{R}} (\epsilon_b - \epsilon_a) \theta(R_s - |\mathbf{r} - \mathbf{R}|), \quad (2)$$

where $\theta(x)$ is the unit step function, $\theta(x) = 1$ for $x \geq 0$ and zero otherwise. The summation is over all dielectric spheres centered at \mathbf{R} and of radius R_s . The dielectric constants of the spheres and the background are, respectively, ϵ_a and ϵ_b , and c is the vacuum speed of light. The classical wave amplitude Ψ and its derivative $\nabla\Psi$ are continuous everywhere.

For our calculations we apply the plane-wave method which is one of the standard methods in the electronic band-structure problem.¹¹ Some aspects of the photon bands have also been discussed by John and Rangarajan^{12,13} using the Korringa-Kohn-Rostoker (KKR) method.

For a periodic arrangement of the spheres $V(\mathbf{r})$ can be expanded in terms of its Fourier components, $V(\mathbf{G})$, where \mathbf{G} is a reciprocal-lattice vector:

$$V(\mathbf{r}) = \sum_{\mathbf{G}} V(\mathbf{G}) e^{i\mathbf{G} \cdot \mathbf{r}}. \quad (3)$$

The wave function $\Psi(\mathbf{r})$ follows the standard Bloch theorem in the electronic structure problem and can be expanded in terms of the plane waves:

$$\Psi_{\mathbf{k}}(\mathbf{r}) = \sum_{\mathbf{G}} C_{\mathbf{G}} e^{i(\mathbf{k} + \mathbf{G}) \cdot \mathbf{r}}, \quad (4)$$

where \mathbf{k} is the Bloch momentum that symmetry labels the wave function. Substituting the Bloch wave function (4) into the Helmholtz equation (1), we find that the expansion coefficients $C_{\mathbf{G}}$ must satisfy the following equa-

tion:

$$\left[|\mathbf{k} + \mathbf{G}|^2 - \frac{\omega^2 \epsilon_b}{c^2} \right] C_G + \sum_{\mathbf{G}'} V(\mathbf{G} - \mathbf{G}') C_{\mathbf{G}'} = 0. \quad (5)$$

For a solution to exist, therefore, the following determinant should be zero:

$$\det \{ H_G \delta_{G, G'} + V_{G, G'} \} = 0, \quad (6)$$

where

$$H_G = |\mathbf{k} + \mathbf{G}|^2 - \omega^2 \epsilon_b / c^2 \quad (7)$$

and

$$V_{G, G'} = V(\mathbf{G} - \mathbf{G}'). \quad (8)$$

Roots of the determinantal equation (6) give at each \mathbf{k} point the photon frequencies ω , i.e., the photon bands.

The inverse Fourier transform of Eq. (3) provides us with the expression for $V(\mathbf{G})$:

$$V(\mathbf{G}) = \frac{1}{\Omega} \int e^{-i\mathbf{G} \cdot \mathbf{r}} V(\mathbf{r}) d^3r, \quad (9)$$

where Ω is the volume of the crystal. On substituting Eq. (2) into Eq. (9), one finds that $V(\mathbf{G})$ depends only on the magnitude $|\mathbf{G}|$, a result that actually holds for any spherically symmetric potential $V(|\mathbf{r}|)$. The Fourier components $V(\mathbf{G})$ are given by

$$V(|\mathbf{G}|) = -\frac{\omega^2}{c^2} (\epsilon_a - \epsilon_b) 3\beta \frac{\sin(GR_s) - GR_s \cos(GR_s)}{(GR_s)^3}, \quad (10a)$$

with the dielectric-sphere packing fraction β given by

$$\beta = \frac{4\pi R_s^3/3}{\Omega_{\text{cell}}}. \quad (10b)$$

Here $G \equiv |\mathbf{G}|$ and Ω_{cell} is the unit-cell volume. Notice that the potential $V(\mathbf{G})$ depends on the photon energy ω unlike in the electronic band problem. Because of this, while in the electron problem the plane-wave method reduces to a matrix diagonalization scheme, here we must follow the computationally slower root-search scheme to solve Eq. (6).

We performed the numerical calculations for the face-centered cubic (fcc) lattice with the dielectric constants varied between ~ 1 and 15. The packing fraction was varied up to $\beta = \pi/3\sqrt{2} \approx 0.74$ corresponding to close packing. In the plane-wave expansion, Eq. (4), we find that retaining ~ 100 plane waves in the summation results in an accuracy better than $< 2\%$ in the calculated photon frequency for the lower-lying modes we are primarily interested here. Test calculations that used ~ 300 plane waves produced negligible differences.

In Fig. 1(a) we show typical photon bands for the fcc structure. The bands are shown along important symmetry lines in the Brillouin zone (BZ) for the case $\epsilon_a = 5, \epsilon_b = 1$, and sphere packing fraction $\beta = 0.15$. Figure

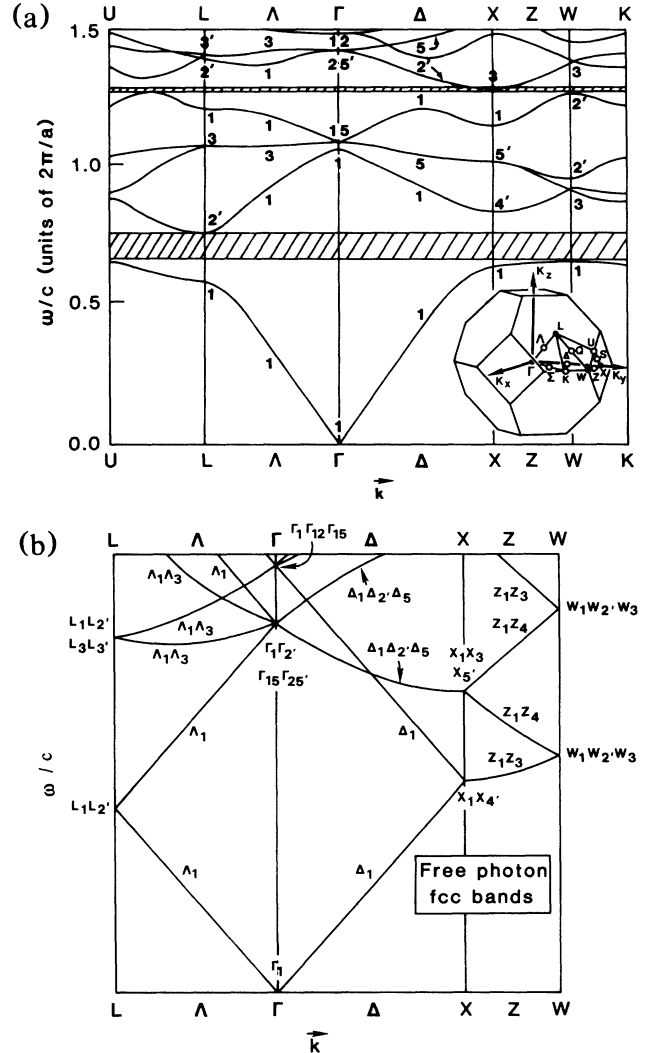


FIG. 1. (a) Typical fcc photon bands calculated in the scalar-wave approximation, compared with (b) the free-photon fcc bands. In (a) $\epsilon_a = 5, \epsilon_b = 1$, and $\beta = 0.15$. The linear dispersion relation, $\omega = \bar{c}k$, is seen in the long-wavelength limit $k \rightarrow 0$ in both cases. The periodic scattering potential modifies the free-photon bands but the various symmetry modes can be identified in (a). The crosshatched areas in (a) show gaps extending throughout the Brillouin zone. Note that the free-photon bands (b) are applicable *both* for the scalar waves as well as for the vector waves satisfying Maxwell's equations. For the vector waves, the free-photon modes with the two distinct helicities are degenerate.

1(b) shows the free-photon fcc modes analogous to the free-electron fcc bands now well known in the electronic band problem. The main difference is the linear dispersion for the photon modes as opposed to the parabolic dispersion relation for the electrons. We have followed the standard Buckaert-Smolukowski-Wigner¹⁴ (BSW) notation for the symmetry classification of various modes. In the long-wavelength limit $k \rightarrow 0$, we see the

linear dispersion relation

$$\omega = \bar{c}k, \tag{11}$$

in the photon bands, where \bar{c} is the average speed of light in the medium,

$$\bar{c} = c/[\beta\epsilon_a + (1 - \beta)\epsilon_b]^{1/2}. \tag{12}$$

The linear dispersion relation, Eq. (11), observed in Ref. 1, follows from Eq. (5) if one retains only the $V(\mathbf{G}=0)$ component, an excellent approximation in the $k \rightarrow 0$ limit.

In the free-photon case, various modes, for instance X_1 and X_4' modes at the X point, $\Gamma_1, \Gamma_2', \Gamma_{15}$, and Γ_{25}' at the Γ point, etc., are degenerate. The degeneracies are removed by the periodic potential that introduces gaps in the spectrum. The magnitude of the gaps at the BZ boundary depends primarily on the magnitudes of certain Fourier components of the potential $V(\mathbf{G})$. In essence, the potential mixes two or more degenerate modes leading to a band splitting, an effect that is illustrated below for the splitting of the X_1 and X_4' modes.

This splitting may be estimated within a nearly-free-photon (NFP) approximation, equivalent to the nearly-free-electron approximation in the band problem. At the

X point, $\mathbf{k} = (2\pi/a)(1,0,0)$, the two free-photon modes, \mathbf{k} and $\mathbf{k} + \mathbf{G}_1$, with $\mathbf{G}_1 = (2\pi/a)(-2,0,0)$, are degenerate in the NFP approximation. The periodic scattering potential removes this degeneracy with the photon frequencies given by Eq. (6), which if we omit the small coupling to the other modes with higher frequencies leads to the condition

$$\det \begin{pmatrix} |\mathbf{k}|^2 - \omega^2/\bar{c}^2 & V(\mathbf{G}_1) \\ V(\mathbf{G}_1) & |\mathbf{k} + \mathbf{G}_1|^2 - \omega^2/\bar{c}^2 \end{pmatrix} = 0, \tag{13}$$

where $|\mathbf{k}| = |\mathbf{k} + \mathbf{G}_1|$ and the Fourier component $V(\mathbf{G})$, given by Eq. (10), contains the photon frequency ω . The coupling of the two modes splits the degeneracy and we have

$$\omega_{\pm} = \omega_0/(1 \pm \lambda)^{1/2}, \tag{14}$$

where $\omega_0 = \bar{c}k$, and λ is a measure of the scattering strength,

$$\lambda = \bar{c}^2 V(\mathbf{G}_1)/\omega^2. \tag{15}$$

The splitting, Eq. (14), corresponds to the gap between the X_1 and X_4' modes in Fig. 1 and it reproduces the results of the full calculation.

In Fig. 2 we show contour plots of $|\Psi_{\mathbf{k}}(\mathbf{r})|^2$ for a few photon modes on the x - y plane. For weak scatterers the photon modes are only slightly perturbed from the free plane waves, an effect that is illustrated in Figs. 2(a) and 2(b) by the contours of the X_1 mode for two different dielectric structures. Inside the dielectric spheres the contours are more densely packed corresponding to the reduction of the speed of light to the value $c/\epsilon_a^{1/2}$. In the rest of Fig. 2 we show the contour plots for important symmetry modes for the case $\epsilon_a = 5.0$ and $\epsilon_b = 1$. The two modes W_1 and L_2' bound the first gap in the frequency spectrum, respectively, from below and above as seen from Fig. 1.

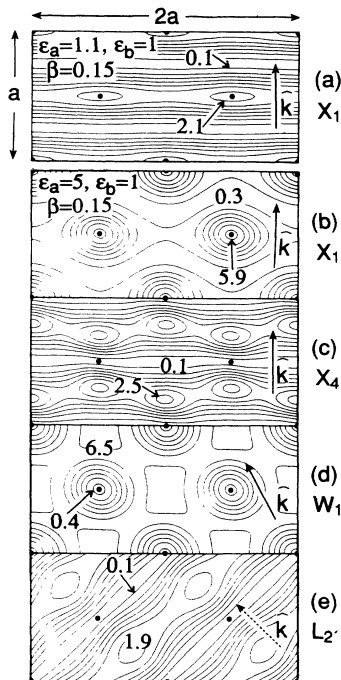


FIG. 2. Contours plots of $|\Psi_{\mathbf{k}}(\mathbf{r})|^2$ for important photon modes in the fcc structure. All contours are on the x - y plane and for packing fraction $\beta = 0.15$. The direction of the \mathbf{k} vector is shown by an arrow except for (e), where its projection is shown. Dots indicate sphere positions. (a),(b) illustrate the gradual evolution of the X_1 mode as the strength of the scatterers is increased. (c)-(e) show contours for selected modes for the case $\epsilon_a = 5$ and $\epsilon_b = 1$.

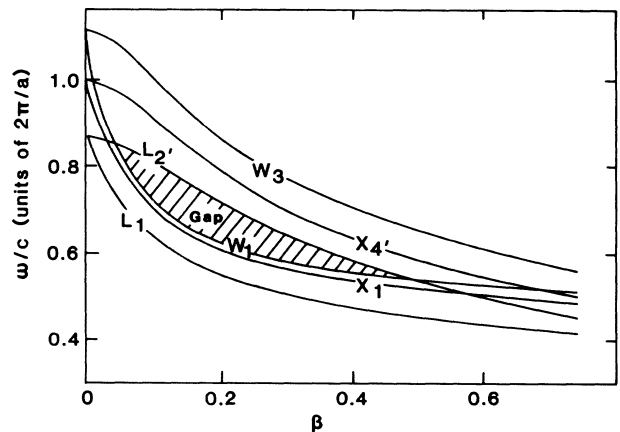


FIG. 3. Variation of the photon frequencies in the region of the lowest gap at high-symmetry points in the Brillouin zone. The crosshatched region indicates existence of a gap in the entire BZ.

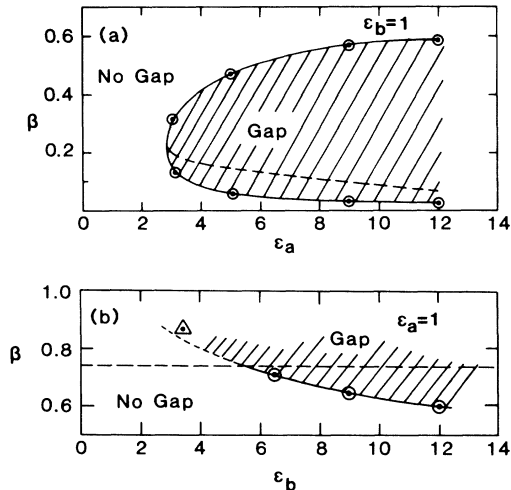


FIG. 4. Condition for the existence of a gap throughout the BZ as a function of ϵ_a , ϵ_b , and β . (a) Case of dielectric spheres packed in vacuum $\epsilon_b = 1$. A gap exists for values of β in the crosshatched area. Outside this range the scatterers are not strong enough to produce a gap in the entire BZ. Below $\epsilon_a \approx 2.8$ there is no gap in the entire range of β . The dashed line in (a) indicates the value of β corresponding to the maximum gap. (b) Case of "air atoms," $\epsilon_a = 1$, with background dielectric constant ϵ_b varied. The numerical calculations were performed up to close packing ($\beta \approx 0.74$); the extrapolation of our results is indicated by the dashed curve in (b). The experimental structure for which a photon gap was reported in Ref. 1 is marked by a triangle.

In Fig. 3 we show the frequencies of various modes in the region of the lowest gap at important symmetry points as a function of the dielectric-sphere packing fraction β for the case $\epsilon_a = 5.0$ and $\epsilon_b = 1$. Results for other dielectric constants are summarized in Fig. 4. Since the case $\beta = 0$ corresponds to a homogeneous dielectric medium with no scatterers, the frequency ω tends to $\omega = c \times |\mathbf{k}| / \epsilon_b^{1/2}$ in this limit. Thus, ϵ_b being equal to 1, at the X , W , and L points, ω/c takes the values 1.0, 1.118, and 0.866, respectively, in units of $2\pi/a$. We find that a gap exists in the entire BZ for β approximately between 0.04 and 0.50 with the maximum value of the gap $\Delta\omega/\omega \approx 10\%$ occurring for the packing fraction $\beta \approx 0.15$. We find that when the gap exists, it is bounded by the W_1 and L_2' modes as seen from Fig. 3. The X_1 mode lies close to the W_1 mode, but always below.

The scattering strength can be varied by changing the dielectric constants ϵ_a and ϵ_b . Figure 4 shows the range of ϵ and β for which our calculations predict existence of

a gap throughout the entire BZ. We find that for $\epsilon_b = 1$, the gap vanishes below $\epsilon_a \approx 2.8$. Above this value of ϵ_a , a gap exists for values of β between two critical values as shown in Fig. 4(a). The case corresponding to the "air atoms" with $\epsilon_a = 1$ and a variable dielectric background ϵ_b is shown in Fig. 4(b) where a gap exists above a critical packing fraction.

We have studied here the nature of photon bands in the scalar-wave approximation, which despite the vector nature of the EM waves is generally found to be adequate in a majority of situations.¹⁵ In fact, the celebrated and very successful diffraction theory of Kirchoff is based on the scalar-wave description only. In spite of this we do expect the vector nature of the EM waves to play a significant role in the photon gaps, an effect that remains to be investigated.

The present work was supported by Grant No. C-3-45417 from the Weldon-Spring Foundation of the University of Missouri. Numerical computations were performed in part at the Pittsburgh Supercomputing Center under Grant No. PHY880084P.

¹E. Yablonovitch and T. J. Gmitter, Phys. Rev. Lett. **63**, 1950 (1989).

²P. W. Anderson, Phys. Rev. **109**, 1492 (1958); Philos. Mag. **B 52**, 5050 (1985).

³S. John, Phys. Rev. Lett. **53**, 2169 (1984).

⁴K. Arya, Z. B. Su, and J. L. Birman, Phys. Rev. Lett. **54**, 1559 (1985).

⁵P. Sheng and Z.-Q. Zhang, Phys. Rev. Lett. **57**, 1879 (1986).

⁶C. A. Condat and T. R. Kirkpatrick, Phys. Rev. Lett. **58**, 226 (1987).

⁷K. Arya, Z. B. Su, and J. L. Birman, Phys. Rev. Lett. **57**, 2725 (1986).

⁸G. Kurizki and A. Z. Genack, Phys. Rev. Lett. **61**, 2269 (1988).

⁹E. Yablonovitch, Phys. Rev. Lett. **58**, 2059 (1987).

¹⁰G. Mie, Ann. Phys. (N.Y.) **25**, 377 (1908); P. Debye, *ibid.* **30**, 57 (1909).

¹¹A general reference for the plane-wave method in the electronic band-structure problem is M. L. Cohen and J. R. Chelikowsky, *Electronic Structure and Optical Properties of Semiconductors* (Springer-Verlag, Berlin, 1987).

¹²S. John, Phys. Rev. Lett. **58**, 2486 (1987).

¹³S. John and R. Rangarajan, Phys. Rev. B **38**, 10101 (1988).

¹⁴L. P. Buckaert, R. Smolukowski, and E. Wigner, Phys. Rev. **50**, 58 (1936).

¹⁵See, for instance, M. Born and E. Wolf, *Principles of Optics* (Pergamon, Oxford, 1965).